

Psychophysical and neurometric detection performance under stimulus uncertainty

Maik C Stüttgen & Cornelius Schwarz

Signal detection theoretical analyses of spike counts have revealed that some cortical neurons can exceed psychophysical sensitivity in cases where a sensory signal is specified exactly. It is not known whether this finding holds in the more natural situation where signal occurrence is temporally uncertain. We investigated the ability of rat barrel cortex neurons to detect faint and transient whisker deflections occurring at unspecified times. The progression from fully specified stimuli to temporal uncertainty degraded neuronal sensitivity such that it seems highly unlikely that single neurons can provide the basis for decoding uncertain perceptual events. However, modeling the sensitivity of neuronal pools on basis of spike timing precision across several neurons in an optimal encoding window of 25 ms showed that the subject's perceptual sensitivity could be based on the occurrence of coincident spikes from four to five neurons.

The question of whether neuronal signaling is reliable depends on the choice of measuring stick. Since early on, investigators have used the performance of the whole subject as a benchmark¹. Many studies since then—most couched in the framework of signal detection theory (SDT)², which allows transformation of neurometric and psychometric data onto the same scale—have corroborated that single neurons in the sensory periphery and in sensory neocortical areas match the precision of the subject (refs. 3–11, reviewed in ref. 8).

These studies clearly set standards for investigating the physiology of perception and made a strong case for the reliability and precision of single units in various areas of the brain. However, SDT analyses assume a 'signal specified exactly'—that everything about the signal is known, including its starting time and duration¹²—which is unlikely to hold in an animal's natural environment. Previous studies used relatively long stimulus presentation times that were often cued and thus well predictable (typically 500 ms to 2 s; for example, see refs. 6,11,13–15). Evolutionary pressure, however, grants that subjects in a natural environment must, at times, process sensory data that are transient, faint in character and uncertain in their time of occurrence. Accordingly, uncertainty about stimulus aspects has been shown to impair psychophysical performance (spatial location¹⁶, stimulus frequency¹⁷ and timing^{18–20}). Another constraint introduced by evolutionary pressure is the need to commit to action as fast as possible after receiving sensory evidence of a potentially dangerous agent, thus leaving time windows as short as tens of milliseconds for sensory processing²¹.

Taken together, it seems important to measure the precision of single neurons under conditions less well specified. In this study, we subjected head-fixed rats to a whisker deflection detection task using transient, faint and temporally uncertain stimuli while monitoring neuronal signals in whisker representations of the primary somatosensory cortex

(barrel cortex) responding to activity in slowly adapting primary afferents. We chose tactile, slowly adapting afferent-driven signals because they feature very long tonic activity (on the order of seconds) in response to transient ramp-and-hold stimuli²², truly challenging properties for the search of fast neuronal processing times (we characterize ramp-and-hold stimuli as 'transient' throughout this paper because, as we will show, only its phasic phase is represented in barrel cortex activity). In addition, to assess neuronal precision in the case of stimulus uncertainty, we tested the hypothesis formulated earlier²³ that, despite the slow adaptation, these signals determine upstream cortical responses and the percept of the animal at a very rapid pace. We took advantage of the fact that slowly and rapidly adapting afferents (the other system of primary afferents present in the rat's tactile whisker system) make up two distinct psychophysical channels that respond to ramp-and-hold whisker deflections drawn from nonoverlapping kinematic ranges²³. Using stimuli that specifically activate the slowly adapting primary afferents, we found that the temporal progression of signals on the level of the barrel cortex driven is indeed very fast. Here we provide arguments that neuronal signaling of transient events under constraints of temporal stimulus uncertainty is likely to rely on the concerted activity of very small pools of neurons generating only a few spikes.

RESULTS

We trained four head-fixed Sprague-Dawley rats to respond to a ramp-and-hold single-whisker deflection by licking at a water spout (Fig. 1a,b). The exact time of stimulus onset was not known to the rat, as it was not explicitly cued, and the interstimulus intervals were drawn at random from a flat probability distribution covering 3.75–6.25 s. Deflection, applied by a piezo bender, was fixed in amplitude at 12°

Hertie-Institute for Clinical Brain Research, Department of Cognitive Neurology, University of Tübingen, 72076 Tübingen, Germany. Correspondence should be addressed to C.S. (cornelius.schwarz@uni-tuebingen.de).

Received 7 April; accepted 13 June; published online 1 August 2008; corrected online 13 August 2008 (details online); doi:10.1038/nn.2162

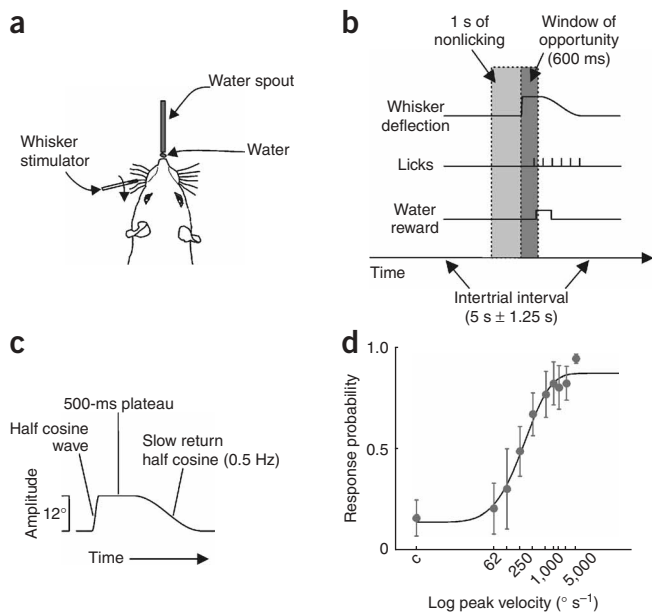


(Fig. 1c), and threshold conditions were achieved by varying the maximal deflection velocity between 62 and $1,500^\circ \text{ s}^{-1}$, presented to the rat in pseudorandom fashion. ‘Catch’ trials (no deflection) were interspersed to monitor random licking in the absence of a stimulus. Using this range of kinematic parameters for deflection, we were able to selectively activate a neuronal subclass of whisker primary sensory fibers, the slowly adapting afferents, up to 750° s^{-1} with minor activation of the other subclass, the rapidly adapting afferents²³. Psychometric detection curves (Fig. 1d; 50% detection achieved around 250° s^{-1}) and the spiking activity of single and multi units in the barrel column receiving the principal input from the stimulated whisker were measured simultaneously in short sessions, guaranteeing that the rat’s motivation was constantly high throughout data acquisition.

The more sensitive barrel cortex single units began to show visually discernible responses in the peristimulus time histograms

Figure 2 Firing properties of barrel cortex neurons and comparison with slowly adapting trigeminal ganglion fibers. (a) Example data from a barrel cortex unit (raster plots and PSTHs). Traces depict stimulus waveforms scaled to the PSTH abscissas. Bottom, PSTHs from a slowly adapting trigeminal ganglion unit for comparison (data from ref. 23). Open arrows point to the phasic response portion. The cortex neuron shows a short-latency response followed by inhibition with higher peak velocities (filled arrow) to stimuli that evoke a phasic response of the slowly adapting primary afferent. Responses to 125° s^{-1} peak velocity were not sampled from the trigeminal ganglion units. (b) Box plots of response widths for single (SU; $n = 18$) and multi (MU; $n = 131$) units. Boxes encompass middle 50% of data-point distributions; whiskers extend to the largest data points or to 1.5 times the interquartile range; + represents outliers; horizontal lines in boxes represent medians. (c) Example PSTH of a slowly adapting ganglion unit at extended time scale to show duration of tonic response component.

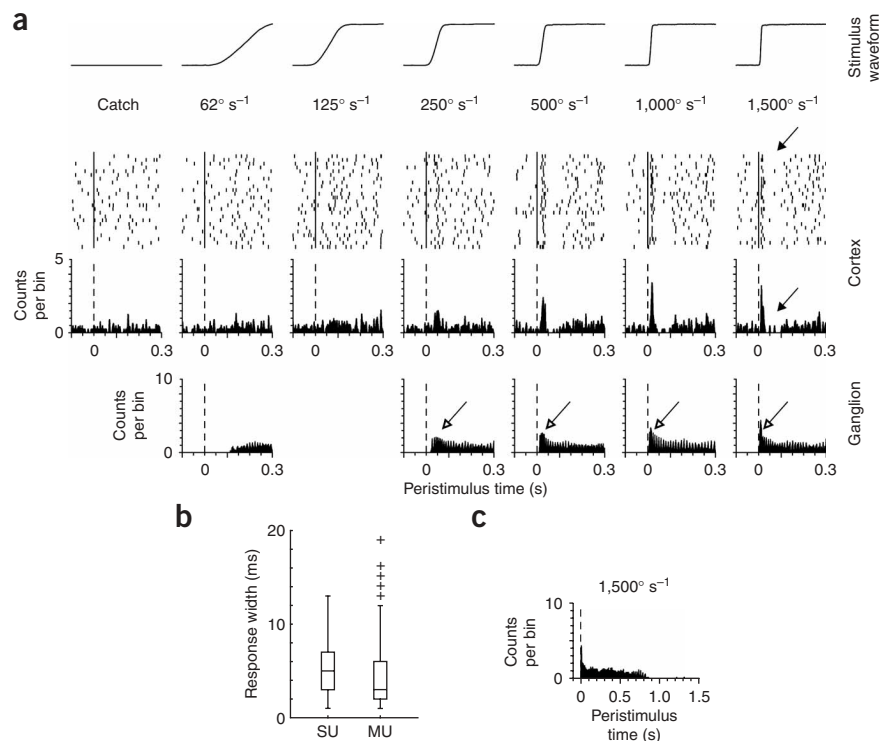


Figure 1 Behavioral protocol and psychometric data. (a) Experimental setup of the head-fixed rat, whisker stimulator and water spout (reward delivery). (b) Behavioral protocol. Licks 1 s before scheduled stimulus onset lead to shift of stimulus presentation by 1 s. A lick within a 600-ms window of opportunity starting from stimulus onset is required to trigger a drop of water as reward. (c) Stimulus waveform. The rat responded to the half cosine wave (deflection in caudal direction). The kinematic parameters of the slow return were far below the detection threshold. (d) Psychometric detection curve as a function of peak deflection velocity. Scale on abscissa is semilogarithmic. Smooth line is a Weibull fit to the psychometric data points, averaged over four rats. Gray circles represent means; error bars represent 95% confidence intervals.

(PSTHs) at a minimum velocity of 250° s^{-1} (Fig. 2a). Despite the salient features of the response in the PSTHs, the spike responses to all stimuli above velocity threshold were extremely sparse, consisting mostly of none, less often of one, and very rarely of more spikes at latencies varying inversely with stimulus velocity. Excitatory responses to higher-velocity stimuli were often followed by a period of inhibition of about 100 ms. Comparison of these responses with those of primary afferents recorded in the trigeminal ganglion in an earlier study²³ revealed that those stimuli that evoked a phasic peak response on top of the tonic response in the trigeminal slowly adapting units also evoked a transient response in the barrel cortex neurons. The width of the excitatory response peaks for an example stimulus is shown in Figure 2b; none of the cortex units we recorded showed an excitatory response longer than 19 ms. This finding holds even though the afferent input to the system, coming from slowly adapting trigeminal ganglion units, responds to ramp-and-hold stimuli in this range with prolonged spiking activity: 10 of 12 slowly adapting ganglion neurons (data reanalyzed from ref. 23) responded for longer than 500 ms (example in Fig. 2c). In summary, these results strongly suggest that only phasic, and not tonic, response components reach the barrel cortex. This is in agreement with previous findings that only the phasic response portion of slowly adapting neurons contributes to the rat’s detection performance²³.

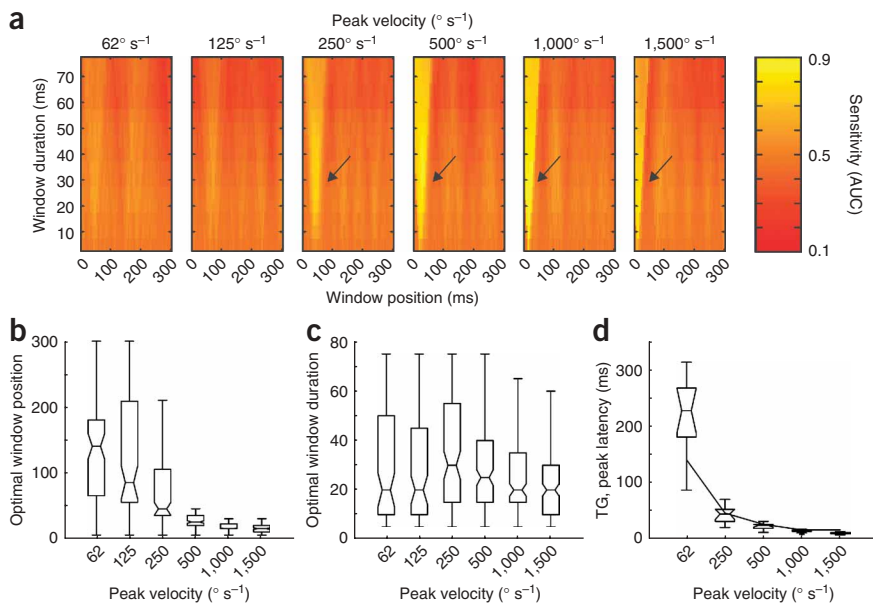


Figure 3 Identification of optimal encoding windows. **(a)** Example neuron from barrel cortex. Each panel depicts the sensitivity of the neuron for each combination of window position (5–300 ms; abscissa) and window duration (5–75 ms; ordinate) for one stimulus velocity. Sensitivity is color-coded, with lighter colors depicting higher values. At low velocities, the panels are basically uniform; with increasing velocity, a yellow stripe appears (arrows), indicating higher sensitivities. **(b)** Box plots of optimal window positions as a function of stimulus velocity. Units included are only those that exceeded their own bootstrapped 95% confidence intervals (see Methods). **(c)** Box plots of optimal window durations as a function of stimulus peak velocity, using same units as in **b**. **(d)** Box plots show latency of peak firing rate in the trigeminal ganglion (TG). For comparison, the median optimal window positions of cortical units (see **b**) is plotted (gray line). Boxes encompass middle 50% of data-point distributions; whiskers extend to the largest data points; horizontal lines represent medians; notches represent 95% confidence intervals of medians.

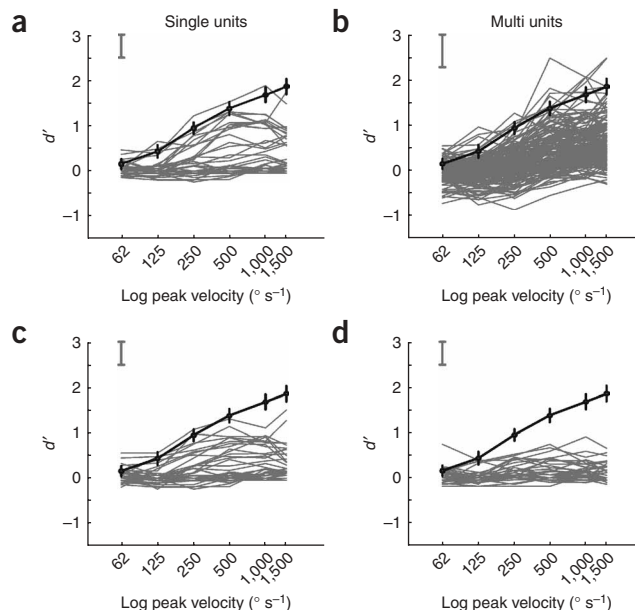
To obtain a quantitative measure of the temporal progression of neuronal sensitivity, we first applied classical SDT analysis, which assumes that the observer has full knowledge about stimulus timing. We then used the resulting information about the temporal evolution of sensitivity and relaxed the assumption of ‘stimulus specified exactly’ to analyze the performance of neurons under the condition of stimulus uncertainty. We calculated a sensitivity index using receiver-operating characteristic (ROC) analysis². In this case, sensitivity can be understood as the probability that an ideal (unbiased) observer can tell the absence or presence of a whisker stimulus (catch trial versus deflection at a certain peak velocity) by looking at single-trial spike counts.

To assess the time window in which the sensitivity of barrel cortex neurons would be optimal, we varied window positions and durations systematically over a large range (position varied 5–300 ms after stimulus onset, duration varied 5–75 ms, both with 5-ms intervals; **Fig. 3a**). To arrive at the best estimate of window position and duration, we extracted the position-duration combination for which the sensitivity index of each unit was maximal (if the index value exceeded the given unit’s bootstrapped 95% confidence interval; see Methods). At peak velocities of 250° s⁻¹ and more, the distributions of optimal window positions (**Fig. 3b**) had a clear unimodal peak with low variability that shifted toward earlier time points with increasing peak velocity of the stimulus (15 ms at 1,500° s⁻¹). The distributions of optimal window durations were relatively constant across stimuli and were centered around 25 ms (**Fig. 3c**). This analysis indicated that spike counts contain maximal information about the presence or absence of a stimulus within a short time window, as might be expected from the low spike counts evoked by stimulation. The latency of the

peak firing rate in trigeminal ganglion cells (**Fig. 3d**) matched quite well the median of the optimal window positions, except for the slowest deflection velocity, where hardly any response was discernible in any of the neurons. Notably, median optimal window positions across stimuli were strongly correlated with the subjects’ average reaction times (ranging from 384 ms for the slowest to 329 ms for the fastest stimulus; Spearman’s $\rho = 0.99$), suggesting that the rats indeed rely on spikes in the first afferent volley to decide whether or not to emit a response.

We next used the median of optimal window positions and durations to obtain the distribution of spike counts for each unit and stimulus, including the catch condition, and calculated the neuronal sensitivity curves (**Fig. 4**). The average sensitivity typically increased with peak velocity of the deflection for both single-unit (**Fig. 4a**) and multi-unit data (**Fig. 4b**). To compare neurometric and psychometric performance, the sensitivities of the rat observers obtained in the same

Figure 4 Psychometric precision acts as upper bound for neurometric precision of barrel cortex neurons. **(a)** Sensitivity of single units ($n = 34$) in barrel cortex as a function of the logarithm of stimulus velocity, expressed as d' (thin gray lines). Bold line represents mean psychometric performance with 95% confidence interval. Vertical gray bars represent extent of average neurometric bootstrapped 95% confidence interval. **(b)** Same as **a** but for multi units ($n = 166$). **(c, d)** Same data as in **a**, but the position of the encoding window was jittered (in a trial-by-trial fashion) by shifts drawn from a Gaussian distribution. **c**, mean = 0, s.d. = 10 ms; **d**, s.d. = 25 ms.



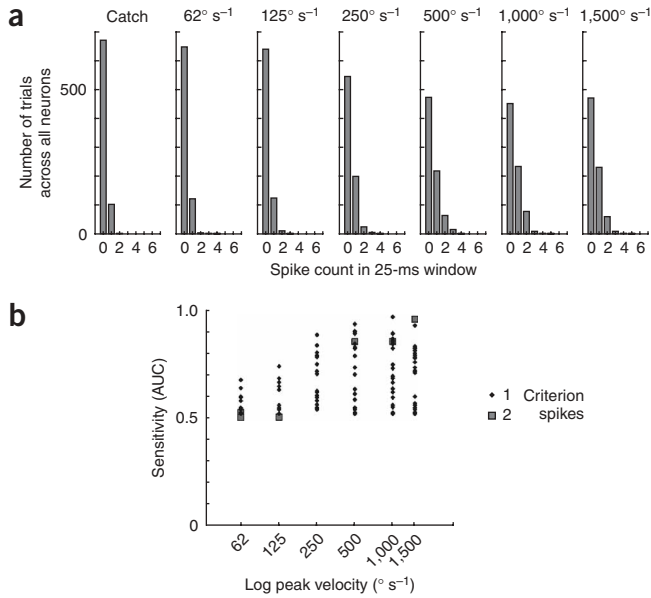


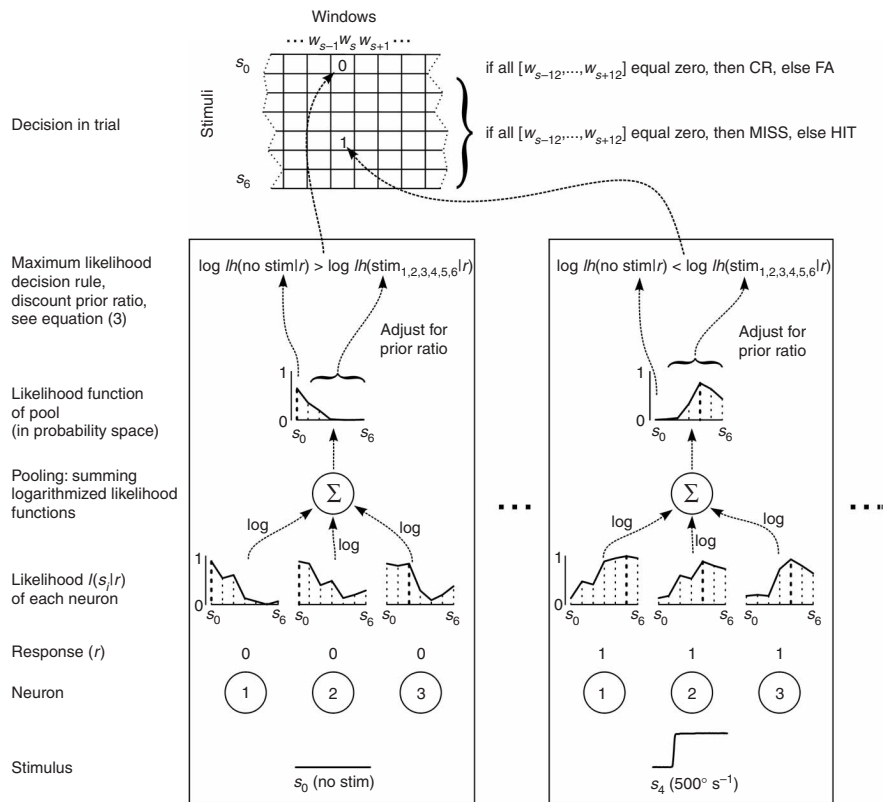
Figure 5 Barrel cortex single units fire low numbers of spikes in response to whisker deflections but may reach high sensitivities. **(a)** Frequency histograms of spike counts in a 25-ms response window at optimal position as a function of deflection velocity (775 trials from 34 single units). **(b)** Optimal criterion spike count of barrel cortex single units ($n = 34$) as a function of stimulus peak velocity and the neurons' sensitivity. Data shown only for neurons with a criterion spike count of at least one.

sessions were plotted on the same axes. The sensitivity curves for both single and multi units were bounded by the psychophysical performance. The proportion of single neurons that showed increasing sensitivity with increasing velocity was 0.76 (26 of 34), as evidenced by d' values exceeding their bootstrapped 95% confidence intervals around 0. The best neurons (one to five neurons, depending on stimulus velocity) just matched the subjects' performance, and only occasionally was a unit found to show slightly higher sensitivity than the subject (maximum overshoot was $\sim 0.3 d'$ units).

It is notable that the ROC analysis averages across all possible criteria of the observer. However, not many criteria were available to the single units in our sample, as their spike count in the 25-ms window was very low. In fact, it consisted mainly of counts of zero and one; two spikes were only observed occasionally, and three spikes were virtually absent (**Fig. 5a**; one of the strongest responses in our sample of single units is shown in **Fig. 2a**). We therefore suspected that the criterion of 'absence or presence' of spikes in the encoding window would contribute most to the performance of the single units. This suspicion was confirmed by searching for the criterion leading to the point in ROC space with maximal classification performance (hit rate minus false alarm rate). Throughout the range of sensitivities present in our set of single units (except near-random performance at sensitivities of 0.5 and a few exceptions in the uppermost sensitivity range, which yielded an optimal criterion of 'two or more'), the best criterion was indeed the presence of one spike or more (**Fig. 5b**).

This finding seemed to suggest that, in principle, the subject could base its decisions on the occurrence of one spike in one of its most sensitive neurons. Before concluding this, however, we considered that the SDT analysis was tuned to yield optimal performance of the neurons. Both the position and duration of the neuronal encoding windows were thus set with full knowledge of exact stimulus timing (at millisecond resolution), whereas in the experimental reality, the rats were deliberately left uncertain about stimulus timing within an

Figure 6 Monte Carlo procedure to estimate sensitivities of neuronal pools. The procedure is shown for two encoding windows (boxes) with different stimuli (no stimulus (s_0), left, and deflection at peak velocity of 500° s^{-1} , right) for a pool of three neurons. In each trial, the window in which the stimulus (s_0 to s_6) was presented (w_s) was determined at random. In each window, the response r of the pool members (absence or presence of spike) was drawn and the log LHF calculated based on the measured response probability of the chosen single units. Response pooling was performed by adding the neurons' LHFs in log space, resulting in the LHF of the pool. Population LHFs of 'stimulus present' (s_1 to s_6) were adjusted discounting the ratio of prior probabilities as given by equation (3) (see Methods) and individually compared to the likelihood of 'stimulus absent' (s_0), thus implementing a winner-takes-all strategy based on the event with maximum likelihood. The decision in the trial was evaluated from the decisions in the 24 windows (600 ms) around stimulus presentation (w_{s-12} to w_{s+11}). In the case of presentation of s_0 , all decisions in the 24 windows were required to be 0 (stimulus absent) to yield a correct rejection (CR). Otherwise, the trial was counted as a false alarm (FA). Likewise, in the case of presentation of one of the whisker deflections (s_1 to s_6), all 24 windows holding zeroes yielded a trial counted as MISS; otherwise it was classified as HIT.



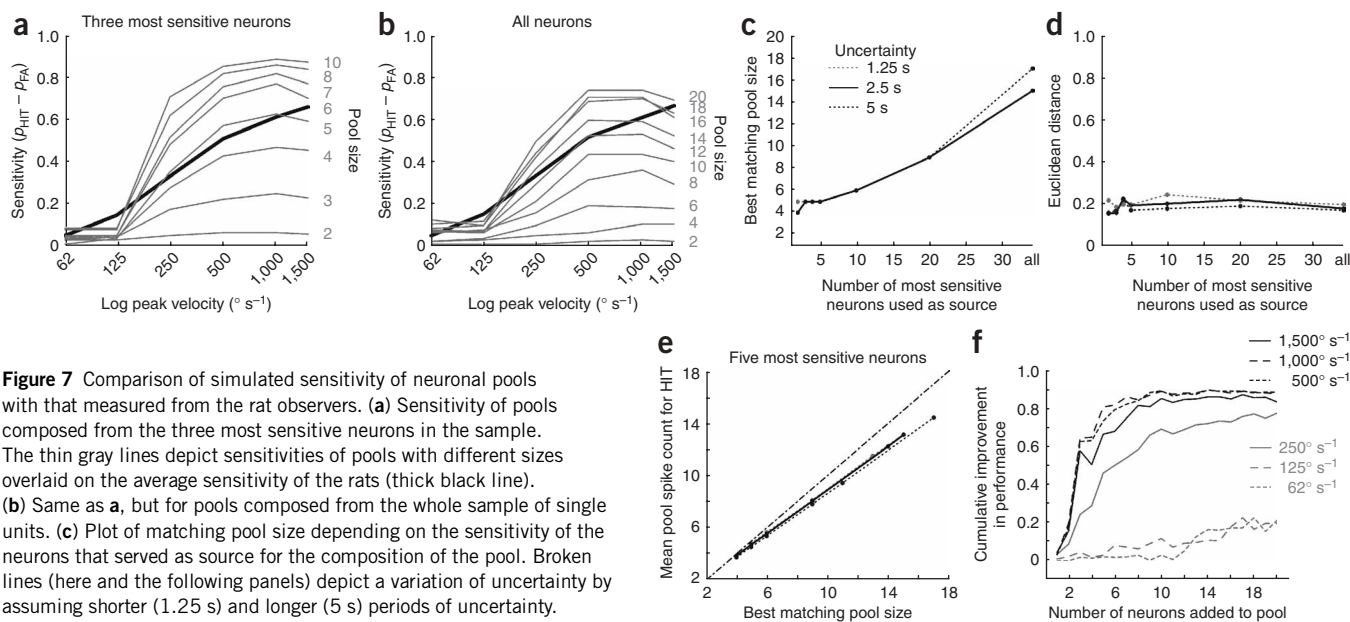


Figure 7 Comparison of simulated sensitivity of neuronal pools with that measured from the rat observers. **(a)** Sensitivity of pools composed from the three most sensitive neurons in the sample. The thin gray lines depict sensitivities of pools with different sizes overlaid on the average sensitivity of the rats (thick black line). **(b)** Same as **a**, but for pools composed from the whole sample of single units. **(c)** Plot of matching pool size depending on the sensitivity of the neurons that served as source for the composition of the pool. Broken lines (here and the following panels) depict a variation of uncertainty by assuming shorter (1.25 s) and longer (5 s) periods of uncertainty. **(d)** Similarity (expressed as Euclidean distance) of sensitivities of rats and the best pools plotted across the data source from which the pool members were chosen. **(e)** Average number of spikes needed to generate a HIT trial. Broken line extending from origin indicates unity. **(f)** Improvement of pool sensitivity if neurons with descending sensitivity are added.

interval of 2.5 s. The importance of knowledge about stimulus timing was revealed by impairing the temporal precision of the encoding window for each trial by adding a random number drawn from a Gaussian curve with a mean of 0 and s.d. of 10 or 25 ms (Fig. 4c,d). Single-neuron sensitivity under these conditions was reduced to values around 0.

A second problem was that knowledge about stimulus time effectively reduces the false alarm rate. For example, the median spontaneous firing rate of single units in our sample was $\sim 6 \text{ spikes s}^{-1}$, which predicts the observation of an average of 0.15 spikes in 25 ms. Given the 'one spike' criterion and the negligible probability of observing two spikes under catch conditions, this seems to correspond nicely to the average response probability of the rat observers of 0.16. The crucial issue is, however, that uncertainty about stimulus timing does not allow the use of a time window fixed to stimulus onset. Rather, the observer is forced to shift an appropriate window through time to gain a running estimate about the sensory environment. Indeed, the one-spike criterion, when applied to the running estimate obtained from shifting 25-ms windows, would clearly be unable to explain the false alarm rate of the rat observer. In fact, the spontaneous firing rate of 6 spikes s^{-1} predicts that a neuron would generate a false alarm probability of close to 1 when shifting a 25-ms window through 600 ms, the window of opportunity that has been applied to measure the rat observer's response to catch stimuli (for example, under the assumption of a Poisson process at 6 Hz, intervals smaller than 600 ms occur at a probability > 0.99). This outcome was not borne out by the observed performance of rats. In summary, we note that the SDT analysis is valuable in yielding an estimate of the temporal progression of neuronal sensitivity, but—given stimulus uncertainty—the comparison of neurometric and psychometric data on the basis of SDT unfairly favors the neuron's performance.

A consequence of these considerations is that the neuron's criterion would need to be elevated from one spike to explain the rat's performance. However, this would immensely reduce the hit rate of single neurons, as even the most sensitive ones hardly fired more than

one spike, even in the presence of a readily detectable high-velocity stimulus (Fig. 5a). There are two possible solutions to this dilemma. The first is to assume that the coding symbol used by barrel cortex neurons goes beyond spike counts and uses some sort of temporal patterning of spikes. We will not explore this possibility further, as the relatively small numbers of trials sampled under the present experimental conditions precluded the quantitative study of such coding schemes²¹. Alternatively, with spike counts as the coding symbol, we must consider a population code; that is, the assumption that the rat's performance is based on more than one spike generated within a pool of neurons. However, because the information-carrying spikes fall in very short (~ 25 -ms) windows, it is necessary to achieve high temporal precision of population spiking to encode the transient stimuli. To arrive at an estimate of the number of neurons and spikes that must be involved to bring neuronal sensitivity to the level of the subject, we built a model that combines the likelihood function (LHF) of neurons within a pool.

As described previously²⁴, the LHF holds the probability of a given neuronal response across stimuli, and thus introduces a statistically optimal weighting of each neuron's contribution to the pool's response according to the quality of its tuning properties (Fig. 6; see Methods for details). We used our sample of 34 high-quality single units and their responses to catch stimulus and the six whisker deflections in each 25-ms window as the data basis for the simulation of neuronal pools and their responses. The uncertainty period was subdivided into 100 windows of 25 ms each. In one of these windows randomly chosen for each trial, one of the seven stimuli (catch and 62 – $1,500^{\circ} \text{ s}^{-1}$) was presented and the LHF for each neuron was calculated. The decision in each 25-ms window was assessed by pooling the neuronal responses by adding the LHF in log space and assessing the stimulus for which maximum likelihood was obtained after discounting prior probabilities of presence or absence of stimuli. In a final step, the decision in a trial was assessed by looking at the pool's decisions in each of the 24 windows that fell within a period of -300 ms to 300 ms to stimulus onset. This was done to mimic the experimental situation in which a

response based on a fake sensory event 300 ms before the stimulus would be placed well into the window of opportunity of the rat, as the response times (decision plus motor preparation and execution) were about 300 ms for high-velocity pulse deflections with ~5-ms response latency in the barrel cortex. One or more decisions in favor of stimulus presentation during this period led to a classification of the trial as 'go' (hit or false alarm) or 'no-go' (miss or correct rejection). The results presented in **Figure 7** are based on 1,000 simulated trials for each stimulus.

The model allowed us to vary the composition of the neuronal pool, from a subset of the most sensitive neurons in the database to all neurons, and the number of neurons in the pool. The effects of these variables on the sensitivity of the model were tested and compared to the actual performance of the rats. The performance of a pool of the three most sensitive neurons in the sample (**Fig. 7a**) was compared to that of a pool that potentially included all neurons in the sample irrespective of their sensitivity (**Fig. 7b**). Pools composed of sensitive neurons were clearly able to match the rat's performance at a much lower pool size than were pools that potentially included all neurons. The minimum matching pool size was 4–5 neurons if only the 2–5 most sensitive neurons were allowed to enter the pool, and reached 15 if all neurons were allowed to contribute (**Fig. 7c**). The amount of uncertainty had a minor role in determining these estimates: between uncertainty periods of 1.25 and 5 s, the numbers of neurons and the closeness of the match required to match the rat's performance remained stable (**Fig. 7c,d**). The number of spikes required to correctly detect a stimulus (hit) depended on the size of the pool that matched the rat's performance. In small matching pools of three to five neurons (typically the ones composed of highly sensitive neurons), basically one spike of every pool member was required for a hit. With larger matching pool sizes (typical for pools that included insensitive neurons), the average criterion for a hit was relaxed to coincident spikes to about 13 of 15 (**Fig. 7e**). Taking the most sensitive neuron first and then adding the neurons according to their order of sensitivity led to a steep improvement of detection performance up to the sixth neuron added. Adding more neurons gave only a minor gain of sensitivity (**Fig. 7f**). In summary, one spike in one highly sensitive neuron is sufficient to explain the subject's detection performance if exact knowledge of stimulus timing is assumed, whereas as few as four to five coincident spikes from as many sensitive neurons are sufficient if this assumption is dropped.

DISCUSSION

Hypotheses about the type of neuronal coding mechanism at work in the sensory cortex should be constrained by taking into account the temporal uncertainty of outside events. To provide a new approach to the question, we investigated whether single-neuron representation could be challenged by presenting highly transient and temporally uncertain stimuli. Using stimulus onset as a reference, high neuronal sensitivity was carried by just one spike within a 25-ms window. Introducing uncertainty led to a marked breakdown of single-neuron sensitivity, for two reasons. First, spontaneous spiking drove neuronal false alarm rates up just short of 100%—greatly at variance with the subject's actual performance. Second, the sparse response of the neurons virtually precluded the generation of more than two spikes in the optimal encoding window. In consequence, with transient and uncertain sensory inputs, the subject's percept is highly unlikely to be supported by a single neuron's spike count. This makes a strong case for the need for weighted pooling of single-neuron information, at least for this class of behavioral tasks.

The sparseness of neuronal responses and the short encoding window suggest that candidate decoding mechanisms use temporal precision of the population response, the spikes' coincidence within 25-ms windows. Temporal precision of coding symbols is expected whenever dynamically changing stimuli are to be encoded^{25–27}. Notably, the optimal information-carrying encoding window of 25 ms and the temporal precision of firing (half-width of response peak around 5 ms) were nearly constant across all stimuli despite greatly varying temporal devolution of deflection kinematics. This temporal precision may be exploited by coincidence mechanisms of receiving cortical networks residing in whole cortical neurons with typical membrane time constants²⁸, or even more precise mechanisms in dendritic branches²⁹.

Here we showed that optimal pooling of only four to five sensitive neurons suffices to match the performance of the rats under conditions of uncertainty. However, our whisker stimuli surely activated a much larger number of neurons in a barrel column, or we would have been unlikely to find any. At first glance, it seems odd that by pooling larger and larger numbers of neurons, neurometric performance is able to exceed that of the subjects by a substantial amount. Does the rat willfully neglect potential information laid down in some hundreds of barrel column neurons by using only a handful of them?

To resolve this discrepancy, it is first important to remember that only a small fraction of neurons in our sample were highly sensitive for the task (3–15%, depending on the stimulus; extrapolated to the number of neurons in a barrel column, this amounts to ~270–1,350 neurons³⁰). It is possible that the fraction of sensitive neurons may decrease even further for more complex problems encountered by animals in their natural environment. Second, monitoring large numbers of neurons may come at a computational cost because large degrees of convergent projections have to be implemented, and pools serving different behavioral tasks are bound to overlap. Moreover, the gain in sensitivity contributed by extra neurons becomes smaller and smaller with increasing pool size (see **Fig. 7f**). The actual pool size for a specific task may therefore be set to a suboptimal level to ensure acceptable overall sensitivity for a large range of behaviorally relevant tasks. Third, while the probabilistic model processes information optimally and noise free, the rat is probably not able to do so. For instance, animals estimate the passage of time with a certain degree of inaccuracy³¹, whereas the model makes perfect adjustments of the probability of stimulus occurrence for each window (a quantity related to the 'hazard rate'; see ref. 31). Finally, results from cortical microstimulation and optogenetic manipulation point to the possibility that, indeed, the activity of small numbers of neurons in barrel cortex can be perceived by the animal^{32,33}.

The present study complements the previous results, as it provides a lower bound of spikes and cells needed to provide sensory evidence to form a percept, based on statistical appraisal of a neuronal pool's sensitivity. Under conditions of temporal uncertainty, the barrel cortex cannot rely on single neurons but may nevertheless use an extremely sparse and temporally precise neuronal code. Our results are thus congruent with the notion that prediction of behavioral outcome from activity in single neurons is fairly low but may be substantially improved after integration in downstream cortical areas^{11,34}. Stimulus uncertainty, the perceptual constraint that gave rise to our notion of the indispensability of neuronal pooling, is the common rule under natural conditions, and the importance of dealing with them as quickly as possible may have had a decisive role in shaping cortical function during evolution. We therefore hold it likely that our results can be generalized to other sensory systems and species and wish to emphasize the importance of studying cortical function under these constraints.

METHODS

Animals. All experimental and surgical procedures were carried out in accordance with standards of the Society of Neuroscience and the German Law for the Protection of Animals. Subjects were four male Sprague-Dawley rats (Harlan Winkelmann), aged 12–16 weeks at the time of implantation.

Chronic implantation of movable multielectrode arrays and recordings.

Anesthesia was introduced with a combination of ketamine and xylazine (100 and 10 mg per kg body weight, respectively) injected intraperitoneally, and maintained with isoflurane (1–2%). The rat was positioned in a stereotaxic apparatus, the skull was exposed and holes were drilled for placement of 11 stainless steel screws. Screws were embedded in dental cement (Heraeus Kulzer). A mounting screw turned upside down was placed in the head-cap. During head-mount surgery, trepanation over the barrel cortex was performed. The C1 barrel was located by mapping the cortex with a single intracerebral electrode. Unit and field potential responses to a brief manual whisker flick were monitored until a site maximally responsive to flicks of whisker C1 with lower activation by flicks of adjacent whiskers was found. Multielectrode arrays (3×3 , 2×3 or 2×2 ; electrode distance, $\sim 250 \mu\text{m}$ to $375 \mu\text{m}$) were centered over the identified location of C1 and slowly inserted into the cortex at a speed of $1.25 \mu\text{m s}^{-1}$ until all electrodes had penetrated the dura (usually 300–800 μm). The electrodes were then slowly retracted to a depth of $\sim 250 \mu\text{m}$ relative to the cortical surface. The cortex was covered with antibiotic ointment, and the electrode array was fixed to the skullcap with dental cement. The wound was treated with antibiotic ointment and sutured. Analgesia and warmth were provided after surgery. Rats were allowed to recover for at least 10 d before habituation training. Rats were housed individually and kept under a 12:12 light-dark cycle with water and food available *ad libitum* except during behavioral testing, when the rats were water-restricted for 5 d per week. Drops in body weight, monitored daily, were prevented by supplementary water.

The movable electrode arrays contained laboratory-built, pulled and ground, glass-coated platinum tungsten electrodes (80 μm shank diameter, 23 μm diameter of the metal core, free tip length $\sim 8 \mu\text{m}$, impedance 2–6 M Ω ; Thomas Recording). Electrode depth could be adjusted by turning a small screw, with one revolution equaling 250 μm . After each successful recording session, we turned the screw by a half revolution until the entire depth of the cerebral cortex was traversed. After that, the screw was turned up maximally and the procedure started again. Voltage traces picked up by the electrodes were bandpass-filtered (200–5,000 Hz) and recorded at a sampling rate of 20 kHz using a multichannel extracellular amplifier (Multi Channel Systems). Spikes were detected using amplitude thresholds. Two-millisecond cutouts centered on the time bin in which the voltage trace first traversed the amplitude threshold were recorded and sorted offline using a laboratory-written software package³⁵. Artifacts were removed and neurons sorted to yield either single- or multi-unit spike trains. Criteria for classification as a single unit were conservative and have been described³⁶. Spontaneous firing rates for each unit were computed from a 500-ms period preceding stimulus onset. We calculated response latencies by measuring the time from stimulus onset (for the reference stimulus) to the time when the firing rate first surpassed a 95% confidence limit, which was computed based on the prestimulus firing rate³⁷. Similarly, we calculated the width of the response peak in the PSTH and, thus, the duration of the excitatory response by measuring the time from the first crossing of the upper 95% significance threshold to the time when the response decreased below the threshold.

Experimental setup and behavioral task. Both the setup and the behavioral task were identical in all aspects to those described in detail elsewhere²³. Briefly, the rats' task was to respond to a brief whisker deflection occurring every 5 s (± 1.25 s) by licking from a water spout. If they emitted a lick response within 600 ms after stimulus onset (reinforcement period, gray field in Fig. 1a), they received a droplet of water as reinforcement. To discourage random licking during the intertrial interval, a period of 1 s without licking was required before a new stimulus would be delivered. In case the rat licked during that period, the scheduled delivery of the next stimulus was delayed by 1 s. Stimulus types were presented in a pseudorandom sequence: the seven stimulus types—deflections of differing velocity and the catch trial—were presented once each in random

sequence before one of them was presented again. Thus, the experiment consisted of n blocks, with all seven stimulus types shuffled and presented once before the seven stimuli were shuffled and presented again.

Optimizing precision of neurometric and psychometric data measurements.

The exact comparison of psychometric and neurometric data has been notoriously difficult, and previous studies show considerable variation. Basically, there is a tradeoff between adjusting the stimulus exactly to the characteristics of the neuron (which favors the neurometric measurement but eventually requires generalization on the animal's side and makes the task harder) and the simplicity of the task (which favors the precision of the psychometric data, but eventually neurons do not get fully engaged; see refs. 6,7,9,13).

To arrive at an optimal balance of both measurements, we used a very simple behavioral task—detection of ramp-and-hold stimuli—and recorded cortical neurons with well-investigated properties in a primary sensory area, the barrel cortex. Parameters that affect neuronal responses in the whisker pathway are receptive field topography, kinematic parameters of the stimulus (amplitude and velocity²³) and directional preference³⁸. The match of topography was ensured by choosing the barrel column corresponding to the deflected whisker (C1) during implantation of the electrodes. In this study, we focused on activity in the barrel cortex that is driven by slowly adapting trigeminal ganglion primary afferents. Thus, the stimulus amplitude was chosen to fully engage these afferents, and peak velocity was varied across the relevant part of their response range²³. For the sake of task constancy, we chose to omit the adjustment of stimulus direction, which in the barrel cortex is weak³⁸. We did so because we wanted to provide a representative sample of barrel cortex units that could be directly compared to each other because they were all measured under identical conditions.

Psychophysical testing was conducted using the method of constant stimuli exactly as described²³, but using only the subset of the stimuli thought to drive mainly the slowly adapting primary afferents. In one session, a set of stimuli of identical amplitude (12°) but differing peak velocities (62°, 125°, 250°, 500°, 1,000° and 1,500°) were presented in pseudorandom order (see above), each for 10–25 times. We then calculated the number of spikes generated by rapidly and slowly adapting units in response to peak velocities of 250–500° using the data in ref. 23. We found that 16 rapidly adapting units fired ~ 0.15 spikes to stimulus velocities of 250–500° s^{-1} at 12°, while 12 slowly adapting afferents confronted with the same stimuli generated ~ 18 spikes (factor 120) within the entire response and ~ 2 spikes (factor 13) in the phasic part of the response. Thus, the separation of responses was near complete in this range. In addition, a catch stimulus was included in which no deflection of the whisker occurred, but lick responses during the reinforcement period were recorded to yield a measure of chance performance (false alarm rate). To check for consistency of performance during the behavioral session, easily detectable reference stimuli (rectangular pulses at amplitude 7°, peak velocity 5,000° s^{-1}) were interspersed with the stimuli of interest. Sessions in which responses to the reference stimulus were below 70%, indicating sloppy performance, were not included in the sample. Regular performance of our rats was much higher, averaging 94%. To ensure optimal performance, we also computed rank-biserial correlations between trial numbers and responses (1 = hit, 0 = miss). A large negative correlation would indicate a constant decrease in responding during the session; the median correlation was -0.12 , indicating that the rats worked steadily. Furthermore, white noise (~ 80 dB) was presented during sessions to ensure that rats responded to tactile input only. In control sessions, the piezo element was disconnected from the whisker but all other experimental variables were kept the same. In these sessions, the rats performed at chance levels, indicating that they did not receive cues other than by tactile whisker deflections.

Data analysis and statistics. Psychophysical data are expressed either as response probability (number of responses divided by number of stimulus presentations) or as the SDT index d' ^{2,12,39}, which conveys the sensitivity of an observer stripped of response bias. Because of the low number of stimulus presentations in this study (10–25 per stimulus type), log-linear corrections were applied to control for response probabilities of 0 and 1 (ref. 39). To compute d' , the response probability for signal trials ('signals' being one of six

different peak velocities) was compared with the response probability for noise trials ('noise' being catch trials) according to the formula $d' = \phi^{-1}(p_{\text{Hit}}) - \phi^{-1}(p_{\text{FA}})$, where ϕ^{-1} is the inverse of the phi function (also called probit function), which converts a probability to a z score, p_{Hit} is the response probability for signal trials (hit rate), and p_{FA} is the response probability for noise trials (false alarm rate).

To achieve comparability with psychometric functions, neurometric detection functions were computed using ROC analysis² as used previously⁴⁰ and more thoroughly described by others⁶. Briefly, spike counts from signal trials were compared with spike counts from noise (catch) trials from the same session. Using a shifting criterion of n spikes, in which n shifts from the minimum spike count to the maximum spike count observed across both trial types, the fraction of both signal and noise trials featuring $\geq n$ spikes was computed. This yielded n measures of hits and false alarms for signal and noise trials, respectively. The area under the ROC curve (AUROC) gives an index of sensitivity, which expresses the amount of overlap between signal and noise (catch) spike count distributions. Sensitivity varies between 0 and 1, with 0.5 indicating complete overlap between the distributions and, thus, nonseparability. Values of 0 and 1, on the other hand, indicate complete separation of the two distributions. To compare psychometric and neurometric functions on the same scale, AUROC was converted to d' using the equation $d' = \phi^{-1}(\text{AUROC})$.

To identify both the optimal duration and position of the spike encoding window, we computed the sensitivity for a range of window duration and position combinations (durations, 5–75 ms; positions, 5–300 ms; both incremented in steps of 5 ms). To arrive at distributions of optimal window positions and durations, we took the duration-position combination at which the sensitivity value was maximal for each given unit, provided that the sensitivity value exceeded a 95% confidence level bootstrapped for each unit individually using spike count distributions taken from the catch trials. As a result, n values for these analyses ranged from 86 units for 62° s^{-1} to 167 units for $1,500^\circ \text{ s}^{-1}$. Throughout, 95% confidence intervals were constructed from t distributions⁴¹ unless stated otherwise.

To model the sensitivity of a neuronal pool, information of single neurons was combined in a statistically optimal way using LHF as described²⁴ (Fig. 6). The LHF holds the probability of a given neuronal response across stimuli. We used our sample of 34 high-quality single units and their responses to catch stimulus and the six whisker deflections in each 25-ms window as the data basis for simulated pools of neurons and their responses. A Monte Carlo procedure was designed to present all seven stimuli (catch, 62 – $1,500^\circ \text{ s}^{-1}$) at a randomly chosen window (w_s) during the uncertainty period (2.5 s, as 100 windows of 25 ms each). The response of each neuron (spike or no spike) in the pool was drawn according to its measured response probability in a 25-ms window centered on the optimal window position for the given stimulus (catch, 0–25 ms after stimulus onset). The LHF holding the likelihood of each of the stimuli given the response (spike or no spike) was then calculated. Next, the LHF of the pool was determined by calculating the likelihood of each stimulus given the particular response pattern. Assuming independence of neuronal responses, this amounts to summing the neuron's logarithmized LHF²⁵. At this point, the uncertainty about stimulus timing was incorporated by accounting for the prior probability of the absence or presence of a stimulus in each window. The decision within the window was formed by sequentially comparing the likelihoods for each stimulus versus 'no' stimulus, on the basis of the following rationale. From the odds form of Bayes' rule, one can derive that it is optimal to decide for hypothesis h_1 versus the alternative h_2 if

$$LR_{1,2} = \frac{1(h_1|r)}{1(h_2|r)} = \frac{p(r|h_1)}{p(r|h_2)} > \frac{p(h_2)}{p(h_1)} = PR_{2,1} \quad (1)$$

that is, if the likelihood ratio of h_1 and h_2 given the response $r(LR_{1,2})$ exceeds the inverse ratio of the respective prior probabilities $PR_{2,1}$ (as in ref. 42, for example). In the present case, the prior ratio is not a constant, but rather decreases with the numbers of past windows in the period of uncertainty, according to

$$PR_{2,1}(w) = 2(w_{\text{tot}} - w + 1) - 1 \quad (2)$$

When calculating the prior ratio for the occurrence of two equally probable stimuli (here, catch versus the given stimulus), w_{tot} is the total number of windows making up the period of uncertainty and w is the running number of the current window. The optimal criterion to decide for the presence of stimulus i (converted to log space) then reads

$$\log(p(r(w)|s_i)) - \log(PR_{2,1}(w)) > \log(p(r(w)|s_{\text{catch}})) \quad (3)$$

where w again represents the w th window and $r(w)$ is the pool response in window w . On the left side of the inequality, $PR_{2,1}$ is accounted for by taking the logarithm and subtracting from the log likelihood of the stimulus (s_i). The right side holds the log likelihood of the catch stimulus given $r(w)$. This procedure was iterated for each of the six whisker stimuli, and the pool's decision was set to 1 ('stimulus present') in one window if any of the six comparisons favored the presence of a stimulus over its absence.

In a final step, the decision in a trial was assessed by looking at the pool's decisions in each of the 24 windows that fell within a period of 600 ms around stimulus presentation (± 300 ms). The rationale was that the rat needs a minimal motor execution time of 300 ms (see Results) and therefore needs to trigger a motor response 300 ms after stimulus onset, at the latest, to emit a lick that falls into the window of opportunity and is thus counted as a response. In addition, 'fake percepts' during the 300 ms before stimulus onset may trigger a response that falls into the window of opportunity. If one or more decisions in favor of stimulus presentation were recorded in this period, the trial was classified as 'go' (hit or false alarm). In case all windows yielded a decision in favor of stimulus absence, the trial was classified as 'no-go' (miss or correct rejection). One run of the simulation repeated this procedure 1,000 times for each stimulus type. For each of such trial, a new combination of neurons was picked from the data source (either the whole sample or varying numbers of the most sensitive neurons; see Results). As there is only one criterion for a decision (spike or no spike) in each encoding window, sensitivities in Figure 7 are expressed as the difference of probabilities of hit and false alarm.

Additional methodological considerations. In the probabilistic model described above, we assumed statistical independence of spike probabilities between subsequent 25-ms windows and between neurons in the pool. In view of the common finding that spike trains from single cortical units often show significant features in autocorrelograms, and that pairs of cortical neurons that are subject to common input can show spike synchrony in the range of tens of milliseconds (typically neurons within one column or related receptive field properties, see for example refs. 43–47), the assumption of independence seems to be an oversimplification. The magnitude of neuronal correlation in the barrel cortex is unknown, particularly under conditions such as our transient stimuli. In cross-correlograms from pairs of cortical neurons, a maximum of ~ 0.1 coincidences per spike at a precision of 10 ms within $\sim 50\%$ of neuronal pairs showing peaks in correlograms has been found⁴⁷. Again, the effect of this correlation—especially on small counts taken from short time windows and small neuronal pools, as is relevant for our main finding—is likely to be negligible. Indeed, it has been shown that the common finding of correlation coefficients around 0.2 for the so-called 'noise correlation' (trial-by-trial covariation of spike counts, for example in ref. 48) is an overestimation resulting from the use of long integration windows^{46,47}. Direct experimental assessment in monkey primary visual cortex revealed that the common value of noise correlation is reduced by more than 75% when using integration windows in the range used here⁴⁹. In summary, considering that the detailed effect of correlation in auto- and cross-correlograms on pool size and spike criterion awaits future measurements that also take possible stimulus-dependent variations of spike correlation into account^{47,50}, we conclude that our simulation is likely to represent a useful first approximation of effective pool sizes and spike criteria.

ACKNOWLEDGMENTS

This work was funded by the Deutsche Forschungsgemeinschaft (SFB550 B11). M.C.S. was supported by a scholarship from the Studienstiftung des deutschen Volkes. We thank F. Jäkel and M. Bethge for helpful discussions concerning signal detection theory and design of the probabilistic model and U. Pascht for excellent technical assistance.

AUTHOR CONTRIBUTIONS

M.C.S. and C.S. designed the experiments; M.C.S. performed the experiments; M.C.S. and C.S. conducted data analyses and wrote the paper.

Published online at <http://www.nature.com/natureneuroscience/>

Reprints and permissions information is available online at <http://npg.nature.com/reprintsandpermissions/>

1. Barlow, H.B. & Levick, W.R. Three factors limiting the reliable detection of light by retinal ganglion cells of the cat. *J. Physiol. (Lond.)* **200**, 1–24 (1969).
2. Tanner, W.P. & Swets, J.A. A decision-making theory of visual detection. *Psychol. Rev.* **61**, 401–409 (1954).
3. Barlow, H.B. Single units and sensation: a neuron doctrine for perceptual psychology? *Perception* **1**, 371–394 (1972).
4. Talbot, W.H., Darian-Smith, I., Kornhuber, H.H. & Mountcastle, V.B. The sense of flutter-vibration: comparison of the human capacity with response patterns of mechanoreceptive afferents from the monkey hand. *J. Neurophysiol.* **31**, 301–334 (1968).
5. Parker, A. & Hawken, M. Capabilities of monkey cortical cells in spatial-resolution tasks. *J. Opt. Soc. Am. A* **2**, 1101–1114 (1985).
6. Britten, K.H., Shadlen, M.N., Newsome, W.T. & Movshon, J.A. The analysis of visual motion: a comparison of neuronal and psychophysical performance. *J. Neurosci.* **12**, 4745–4765 (1992).
7. Celebrini, S. & Newsome, W.T. Neuronal and psychophysical sensitivity to motion signals in extrastriate area MST of the macaque monkey. *J. Neurosci.* **14**, 4109–4124 (1994).
8. Parker, A.J. & Newsome, W.T. Sense and the single neuron: probing the physiology of perception. *Annu. Rev. Neurosci.* **21**, 227–277 (1998).
9. Geisler, W.S. & Albrecht, D.G. Visual cortex neurons in monkeys and cats: detection, discrimination, and identification. *Vis. Neurosci.* **14**, 897–919 (1997).
10. Hernandez, A., Zainos, A. & Romo, R. Neuronal correlates of sensory discrimination in the somatosensory cortex. *Proc. Natl. Acad. Sci. USA* **97**, 6191–6196 (2000).
11. de Lafuente, V. & Romo, R. Neuronal correlates of subjective sensory experience. *Nat. Neurosci.* **8**, 1698–1703 (2005).
12. Swets, J.A. Detection theory and psychophysics: a review. *Psychometrika* **26**, 49–63 (1961).
13. Purushothaman, G. & Bradley, D.C. Neural population code for fine perceptual decisions in area MT. *Nat. Neurosci.* **8**, 99–106 (2005).
14. Uka, T. & DeAngelis, G.C. Contribution of middle temporal area to coarse depth discrimination: comparison of neuronal and psychophysical sensitivity. *J. Neurosci.* **23**, 3515–3530 (2003).
15. Heuer, H.W. & Britten, K.H. Optic flow signals in extrastriate area MST: comparison of perceptual and neuronal sensitivity. *J. Neurophysiol.* **91**, 1314–1326 (2004).
16. Cohn, T.E. & Lasley, D.J. Detectability of a luminance increment: effect of spatial uncertainty. *J. Opt. Soc. Am.* **64**, 1715–1719 (1974).
17. Swets, J.A., Shipley, E.F., McKey, M.J. & Green, D.M. Multiple observations of signals in noise. *J. Opt. Soc. Am.* **31**, 514–521 (1959).
18. Green, D.M. & Weber, D.L. Detection of temporally uncertain signals. *J. Acoust. Soc. Am.* **67**, 1304–1311 (1980).
19. Green, D.M. & Forrester, T.G. Temporal gaps in noise and sinusoids. *J. Acoust. Soc. Am.* **86**, 961–970 (1989).
20. Lasley, D.J. & Cohn, T. Detection of a luminance increment: effect of temporal uncertainty. *J. Opt. Soc. Am.* **71**, 845–850 (1981).
21. de Ruyter van Steveninck, R.R. & Bialek, W. Reliability and statistical efficiency in a blowfly movement-sensitive neuron. *Phil. Trans. R. Soc. Lond. B* **348**, 321–340 (1995).
22. Gibson, J.M. & Welker, W.I. Quantitative studies of stimulus coding in first-order vibrissa afferents of rats. 2. Adaptation and coding of stimulus parameters. *Somatosens. Res.* **1**, 95–117 (1983).
23. Stüttgen, M.C., Rüter, J. & Schwarz, C. Two psychophysical channels of whisker deflection in rats align with two neuronal classes of primary afferents. *J. Neurosci.* **26**, 7933–7941 (2006).
24. Jazayeri, M. & Movshon, J.A. Optimal representation of sensory information by neural populations. *Nat. Neurosci.* **9**, 690–696 (2006).
25. Theunissen, F. & Miller, J.P. Temporal encoding in nervous systems: a rigorous definition. *J. Comput. Neurosci.* **2**, 149–162 (1995).
26. Mainen, Z.F. & Sejnowski, T.J. Reliability of spike timing in neocortical neurons. *Science* **268**, 1503–1506 (1995).
27. Hunter, J.D., Milton, J.G., Thomas, P.J. & Cowan, J.D. Resonance effect for neural spike time reliability. *J. Neurophysiol.* **80**, 1427–1438 (1998).
28. Shadlen, M.N. & Newsome, W.T. Noise, neural codes and cortical organization. *Curr. Opin. Neurobiol.* **4**, 569–579 (1994).
29. Ariav, G., Polsky, A. & Schiller, J. Submillisecond precision of the input-output transformation mediated by fast sodium dendritic spikes in basal dendrites of CA1 pyramidal neurons. *J. Neurosci.* **23**, 7750–7758 (2003).
30. de Kock, C.P.J., Bruno, R.M., Spors, H. & Sakmann, B. Layer- and cell-type-specific suprathreshold stimulus representation in rat primary somatosensory cortex. *J. Physiol. (Lond.)* **581**, 139–154 (2007).
31. Janssen, P. & Shadlen, M.N. A representation of the hazard rate of elapsed time in macaque area LIP. *Nat. Neurosci.* **8**, 234–241 (2005).
32. Huber, D. *et al.* Sparse optical microstimulation in barrel cortex drives learned behaviour in freely moving mice. *Nature* **451**, 61–64 (2008).
33. Houweling, A.R. & Brecht, M. Behavioural report of single neuron stimulation in somatosensory cortex. *Nature* **451**, 65–68 (2008).
34. de Lafuente, V. & Romo, R. Inaugural Article: Neural correlate of subjective sensory experience gradually builds up across cortical areas. *Proc. Natl. Acad. Sci. USA* **103**, 14266–14271 (2006).
35. Hermle, T., Schwarz, C. & Bogdan, M. Employing ICA and SOM for spike sorting of multielectrode recordings from CNS. *J. Physiol. (Paris)* **98**, 349–356 (2004).
36. Mock, M., Butovas, S. & Schwarz, C. Functional unity of the ponto-cerebellum: evidence that intrapontine communication is mediated by a reciprocal loop with the cerebellar nuclei. *J. Neurophysiol.* **95**, 3414–3425 (2006).
37. Abeles, M. Quantification, smoothing, and confidence limits for single-units' histograms. *J. Neurosci. Methods* **5**, 317–325 (1982).
38. Simons, D.J. & Carvell, G.E. Thalamic cortical response transformation in the rat vibrissa/barrel system. *J. Neurophysiol.* **61**, 311–330 (1989).
39. Stanislaw, H. & Todorov, N. Calculation of signal detection theory measures. *Behav. Res. Methods Instrum. Comput.* **31**, 137–149 (1999).
40. Barlow, H.B., Levick, W.R. & Yoon, M. Responses to single quanta of light in retinal ganglion cells of the cat. *Vision Res. Suppl* **3**, 87–101 (1971).
41. Cumming, G. & Finch, S. A primer on the understanding, use, and calculation of confidence intervals that are based on central and noncentral distributions. *Educ. Psychol. Meas.* **61**, 532–574 (2001).
42. Lindley, D.V. *Making Decisions*. (John Wiley & Sons, New York, 1971).
43. Michalski, A., Gerstein, G.L., Czarkowska, J. & Tarnecki, R. Interactions between cat striate cortex neurons. *Exp. Brain Res.* **51**, 97–107 (1983).
44. Ts'o, D.Y., Gilbert, C.D. & Wiesel, T.N. Relationships between horizontal interactions and functional architecture in cat striate cortex as revealed by cross-correlation analysis. *J. Neurosci.* **6**, 1160–1170 (1986).
45. Schwarz, C. & Bolz, J. Functional specificity of a long-range horizontal connection in cat visual cortex: a cross-correlation study. *J. Neurosci.* **11**, 2995–3007 (1991).
46. Bair, W., Zohary, E. & Newsome, W.T. Correlated firing in macaque visual area MT: time scales and relationship to behavior. *J. Neurosci.* **21**, 1676–1697 (2001).
47. Kohn, A. & Smith, M.A. Stimulus dependence of neuronal correlation in primary visual cortex of the macaque. *J. Neurosci.* **25**, 3661–3673 (2005).
48. Zohary, E., Shadlen, M.N. & Newsome, W.T. Correlated neuronal discharge rate and its implications for psychophysical performance. *Nature* **370**, 140–143 (1994).
49. Reich, D.S., Mechler, F. & Victor, J.D. Independent and redundant information in nearby cortical neurons. *Science* **294**, 2566–2568 (2001).
50. Vaadia, E. *et al.* Dynamics of neuronal interactions in monkey cortex in relation to behavioural events. *Nature* **373**, 515–518 (1995).